Title
Impact of Frictional Interactions on Conductivity, Diffusion, and Transference Number in Ether- and Perfluoroether-Based Electrolytes

Journal
Journal of The Electrochemical Society, 167(12)

ISSN
0013-4651

Authors
Grundy, Lorena S
Shah, Deep B
Nguyen, Hien Q
et al.

Publication Date
2020-01-09

DOI
10.1149/1945-7111/abb34e

Peer reviewed

Impact of Frictional Interactions on Conductivity, Diffusion, and Transference Number in Ether- and Perfluoroether-Based Electrolytes

Journal of The Electrochemical Society, 2020 **167** 120540

Impact of Frictional Interactions on Conductivity, Diffusion, and Transference Number in Ether- and Perfluoroether-Based Electrolytes

Lorena S. Grundy,[1,2,=] Deep B. Shah,[1,2,3,=] Hien Q. Nguyen,[1,2] Kyle M. Diederichsen,[1,4] Hasan Celik,[1] Joseph M. DeSimone,[5,6] Bryan D. McCloskey,[1,4,*] and Nitash P. Balsara[1,2,3,*,z]

[1]*Department of Chemical and Biomolecular Engineering, University of California, Berkeley, Berkeley, California 94720, United States of America*
[2]*Joint Center for Energy Storage Research (JCESR), Lawrence Berkeley National Lab, Berkeley, California 94720, United States of America*
[3]*Materials Sciences Division, Lawrence Berkeley National Lab, Berkeley, California 94720, United States of America*
[4]*Energy Storage and Distributed Resources Division, Lawrence Berkeley National Lab, Berkeley, California 94720, United States of America*
[5]*Department of Chemistry, University of North Carolina at Chapel Hill, Chapel Hill, North Carolina 27599, United States of America*
[6]*Department of Chemical and Biomolecular Engineering, North Carolina State University, Raleigh, North Carolina 27695, United States of America*

There is growing interest in fluorinated electrolytes due to their high-voltage stability. We use full electrochemical characterization based on concentrated solution theory to investigate the underpinnings of conductivity and transference number in tetraglyme/LiTFSI mixtures (H4) and a fluorinated analog, C8-DMC, mixed with LiFSI (F4). Conductivity is significantly lower in F4 than in H4, and F4 exhibits negative cation transference numbers, while that of H4 is positive at most salt concentrations. By relating Stefan-Maxwell diffusion coefficients, which quantify ion-solvent and cation-anion frictional interactions, to conductivity and transference number, we determine that at high salt concentrations, the origin of differences in transference number is differences in anion-solvent interactions. We also define new Nernst-Einstein-like equations relating conductivity to Stefan-Maxwell diffusion coefficients. In H4 at moderate to high salt concentrations, we find that all molecular interactions must be included. However, we demonstrate another regime, in which conductivity is controlled by cation-anion interactions. The applicability of this assumption is quantified by a pre-factor, β_{+-}, which is similar to the "ionicity" pre-factor that is often included in the Nernst-Einstein equation. In F4, β_{+-} is unity at all salt concentrations, indicating that ionic conductivity is entirely controlled by the Stefan-Maxwell diffusion coefficient quantifying cation-anion frictional interactions.

 [DOI: 10.1149/1945-7111/abb34e]

Manuscript submitted June 12, 2020; revised manuscript received August 10, 2020. Published September 10, 2020.

Supplementary material for this article is available online

List of Symbols

a	fit parameter in Eq. 5
b	fit parameter in Eq. 5
c	salt concentration (mol cm^{-2})
c_0	solvent concentration (mol cm^{-2})
c_T	total concentration (mol cm^{-2}) ($c_0 + 2c$ for univalent salts)
D	salt mutual diffusion coefficient (cm^2 s^{-1})
D_{self}	salt mutual diffusion coefficient estimated from NMR self-diffusion coefficient values (cm^2 s^{-1}) (Eq. 11)
$D_{self,+}$	cation self-diffusion coefficient measured by PFG-NMR (cm^2 s^{-1})
$D_{self,-}$	anion self-diffusion coefficient measured by PFG-NMR (cm^2 s^{-1})
$D_{self,0}$	solvent self-diffusion coefficient measured by PFG-NMR (cm^2 s^{-1})
$\mathfrak{D}$	salt diffusion coefficient based on a thermodynamic driving force (cm^2 s^{-1}) (Eq. 12)
$\mathfrak{D}_{ij}$	Stefan-Maxwell diffusion coefficient describing interactions between components i and j, which can be the cation, anion, or solvent (cm^2 s^{-1})
$\mathfrak{D}_{0+}$	Stefan-Maxwell diffusion coefficient describing interactions between cation and solvent (cm^2 s^{-1})
$\mathfrak{D}_{0-}$	Stefan-Maxwell diffusion coefficient describing interactions between anion and solvent (cm^2 s^{-1})
$\mathfrak{D}_{+-}$	Stefan-Maxwell diffusion coefficient describing interactions between cation and anion (cm^2 s^{-1})
E	NMR signal attenuation
F	Faraday's constant (96,485 C mol^{-1})
FSI^-	bis(fluorosulfonyl)imide
F4	mixtures of C8-DMC and LiFSI salt
g	magnetic field gradient strength (T/m)
H4	mixtures of tetraglyme and LiTFSI salt
I_{ss}	steady-state current (mA)
I_Ω	initial current calculated using Ohm's law (mA) ($I_\Omega = \Delta V/R_T$)
k_0	offset voltage (V)
l	thickness of electrolyte (cm)
Li^+	lithium cation
m	salt molality (mol kg^{-1})
$t_{+,NMR}$	transference number obtained using PFG-NMR (Eq. 2)
t_+^0	transference number obtained using the Balsara and Newman method
R	ideal gas constant (8.3145 J mol^{-1} K^{-1})
R_{ss}	steady-state cell resistance (Ω)
R_T	total cell resistance (Ω)
R_0	initial cell resistance (Ω)

[=]These authors contributed equally to this work.
*Electrochemical Society Member.
[z]E-mail: nbalsara@berkeley.edu

T	temperature (30 °C everywhere in this study)
$TFSI^-$	bis(trifluoromethanesulfonyl)imide anion
x_{salt}	mole fraction of salt
z_+	cation charge number (1 for univalent salts)
z_-	anion charge number (−1 for univalent salts)

Greek

β_{self}	conductivity pre-factor from the Nernst-Einstein equation (Eq. 1)
β_{+-}	conductivity pre-factor from Eq. 21
β_0	conductivity pre-factor from Eq. 22
$\beta_{0,c}$	conductivity pre-factor from Eq. 23
γ	gyromagnetic ratio (rad s^{-1} T^{-1})
$\gamma_\pm$	molal salt activity coefficient
δ	PFG-NMR magnetic field gradient pulse length (ms)
Δ	PFG-NMR diffusion delay (s)
ΔV	applied polarization potential (V)
η	viscosity (Pa s)
κ	ionic conductivity (S cm^{-1})
ν_+	cations per molecule of salt (1 for univalent salts)
ν_-	anions per molecule of salt (1 for univalent salts)
ν	total number of ions into which the salt dissociates (2 for univalent salts)
ρ_+	current fraction obtained using the steady-state current method (Eq. 4)
τ	separator tortuosity
τ_d	delay for gradient recovery in PFG-NMR (s) (Eq. 9)

The electrolyte used in current lithium-ion batteries is a mixture of ethylene carbonate (EC) and dimethyl carbonate (DMC), and a lithium salt, lithium hexafluorophosphate ($LiPF_6$).[1–3] There is growing interest in developing electrolytes for new battery chemistries that cannot be supported by this mixture.[4] One approach for improving the energy density of rechargeable batteries is by increasing the operating voltage of the cell. EC/DMC/$LiPF_6$ is neither stable against lithium metal nor is it stable against next-generation high-voltage lithium transition metal oxide cathode materials, in particular those with high nickel content.[1,5,6] There is thus considerable interest in ether-based electrolytes, such as poly (ethylene oxide) (PEO), which are stable against lithium metal.[7–10] Similarly, there is emerging interest in developing electrolytes based on fluorinated solvents due to their high-voltage stability.[11–15] Electrolyte performance depends crucially on ion solvation. In both carbonate- and ether-based electrolytes, the lithium cations are coordinated with the electronegative oxygen atoms on the solvent molecules.[7,9] Relatively little is known about the nature of ion solvation in fluorinated electrolytes. It is well-known that fluorinated compounds are highly soluble in one another, which is often referred to as the fluorous effect.[16] One might expect this effect to strengthen coordination between fluorinated anions and the fluorinated solvent. In addition to these effects, electrolyte performance depends on interactions between the non-coordinated ion and the solvent, and cation-anion interactions.[17,18]

At the continuum level, ion transport in binary electrolytes, which are composed of a solvent and two ions, is governed by three Stefan-Maxwell diffusion coefficients that quantify inverse frictional interactions between the cation and the solvent, $\mathfrak{D}_{0+}$, the anion and the solvent, $\mathfrak{D}_{0-}$, and the cation and the anion, $\mathfrak{D}_{+-}$, as well as a thermodynamic factor.[19] Methods to measure these quantities have been established in the literature and have been applied to several systems.[20–22] It is convenient to measure the thermodynamic factor and three related transport properties: ionic conductivity, κ, salt diffusion coefficient, D, and the transference number, t_+^0, and use well-established relationships to obtain Stefan-Maxwell diffusion coefficients from these measurements.[23]

Measurements of ion self-diffusion coefficients, $D_{self,+}$ and $D_{self,-}$, by pulsed-field gradient NMR (PFG-NMR) have provided valuable insight into the underpinnings of ion transport.[24–32] In ideal, dilute electrolytes, wherein the activity coefficients of the ions are unity, the relationships between self-diffusion coefficients and ion transport coefficients are relatively simple. In this limit, ionic conductivity is given by the Nernst-Einstein equation, which is often modified to give Eq. 1,

$$\kappa = \beta_{self}\frac{cF^2}{RT}(z_+^2\nu_+D_{self,+} + z_-^2\nu_-D_{self,-}), \quad [1]$$

where z_+ and z_- are the charge numbers, ν_+ and ν_- are the number of cations and anions, c is the salt concentration, and F is Faraday's constant.[19] The parameter β_{self} is a pre-factor that relates ion self-diffusion coefficients to conductivity. The inverse of β_{self} is often referred to as the Haven ratio.[33,34] In ideal dilute electrolytes, β_{self} is unity, and thus ionic conductivity is entirely dependent on the self-diffusion coefficients of the ions. In this limit, self-diffusion coefficients are inversely proportional to viscosity via the Stokes-Einstein relation.[35] If this relationship is assumed to hold at all salt concentrations, one obtains the Walden plot wherein data from different electrolytes collapse onto a line when conductivity is plotted against the reciprocal of viscosity.[27,36,37] In the literature, β_{self} is often called ionicity, and is assumed to reflect the extent of salt dissociation in the electrolyte.[26–29,33,38–40] However, many lithium battery electrolytes are far from ideal, even in the dilute limit. It is therefore not surprising to find that experimentally-determined values of κ, c, $D_{self,+}$, and $D_{self,-}$ do not obey Eq. 1, even in relatively dilute systems.[26–29,33,38–41]

Many recent publications emphasize the importance of another transport property, the transference number.[25,29,42–49] In seminal work in 1987, Bruce and Vincent proposed a simple method for measuring the transference number.[50,51] They recognized that the transference number thus obtained is correct only in the case of ideal dilute electrolytes. In this case, the cation transference number obtained by the Bruce-Vincent method is identical to that based on self-diffusion coefficients, given in Eq. 2,

$$t_{+,NMR} = \frac{z_+D_{self,+}}{z_+D_{self,+} - z_-D_{self,-}}, \quad [2]$$

in which the subscript NMR is used because PFG-NMR is often used to measure the self-diffusion coefficients. One may consider Eqs. 1 and 2 as characteristic of ideal dilute electrolytes. The rigorously-defined cation transference number with respect to the solvent velocity, t_+^0, however, is given by Eq. 3,[19]

$$t_+^0 = \frac{z_+\mathfrak{D}_{0+}}{z_+\mathfrak{D}_{0+} - z_-\mathfrak{D}_{0-}}. \quad [3]$$

While $t_{+,NMR}$ and that measured by the Bruce-Vincent method must be positive, there are several instances of negative t_+^0 values, as measured using electrochemical techniques[21,22,52,53] as well as using electrophoretic NMR.[25]

The objective of this paper is to quantify the relationships between the different ion transport properties introduced above. We have chosen two model systems: a conventional ether-based electrolyte comprised of tetraglyme and lithium bis(trifluoromethanesulfonyl) imide (LiTFSI), and a fluorinated analog, a perfluoroether-based electrolyte comprised of C8-DMC and lithium bis(fluorosulfonyl) imide (LiFSI). The chemical structures of the solvents and salts are shown in Fig. 1. Both solvents contain four repeat units and differ mainly in the fact that C8-DMC is fluorinated. We thus refer to the two systems as "H4" and "F4," respectively. F4 is expected to have a lower dielectric constant than H4.[54] We note that the end-groups of H4 and F4 are different. Finally, we also note that different anions were used ($TFSI^-$ in H4 and FSI^- in F4). FSI was chosen in F4 because it led to a higher ionic conductivity.[55] We compare thermodynamic factors, continuum transport properties, and self-diffusion coefficients measured in the two systems. Both systems are complex, and conductivity is not well-described by Eq. 1. We use concentrated solution theory[19] to arrive at analogous equations that relate conductivity to Stefan-Maxwell diffusion coefficients rather than self-diffusion coefficients.

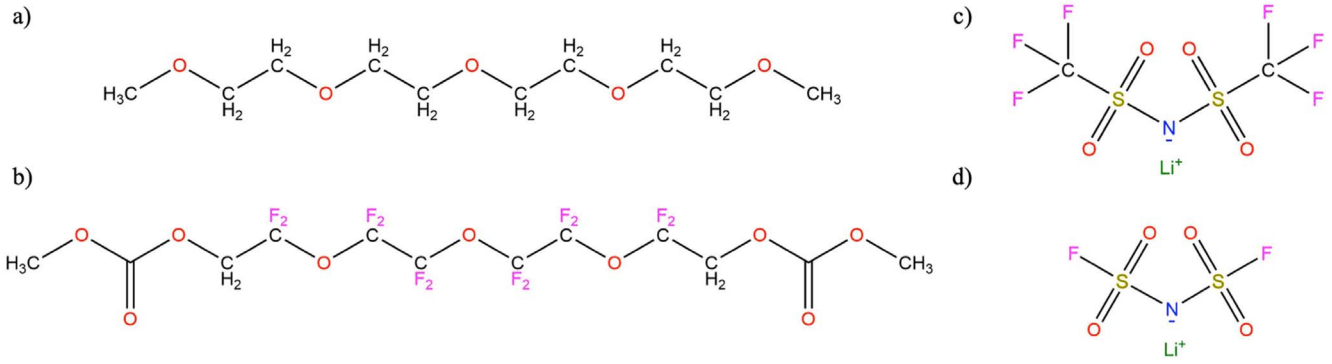

Figure 1. Chemical structures of tetraglyme (a), C8-DMC (b), LiTFSI (c), and LiFSI (d).

These relationships are essential for understanding the origin of differences in ion transport in H4 and F4.

An important objective of this study is to answer the following questions:

(1) Are differences in conductivity in H4 and F4 related to differences in ion self-diffusion coefficients, $D_{self,+}$ and $D_{self,-}$, as anticipated by Eq. 1?
(2) Are differences in conductivity in H4 and F4 related to differences in viscosity?
(3) Is β_{self} a measure of the extent of ion dissociation in H4 and F4?

Methods

Electrolyte preparation.—C8-DMC was synthesized from a diol-terminated precursor as described elsewhere and has a molecular weight of 526 g mol^{-1}.[54,56] Tetraglyme was purchased from Sigma Aldrich. Both polymers were dried under dynamic vacuum at 50 °C for three days. LiFSI and LiTFSI were purchased from Oakwood Products, Inc. and Sigma Aldrich, respectively. Salts were dried under dynamic vacuum at 100 °C for three days. In an Ar glovebox, Li salt was added to the respective polymer by mass and mixed using a magnetic stirrer for at least 12 h. Figure 1 shows the chemical structures of tetraglyme (a), C8-DMC (b), LiTFSI (c), and LiFSI (d). Mixtures of tetraglyme (a) and LiTFSI (c) are denoted as "H4" and mixtures of C8-DMC (b) and LiFSI (d) are denoted as "F4." LiFSI was used in F4 because previous work found it to be the salt that resulted in the highest conductivity in C8-DMC-based electrolytes.[55] Table I shows conversions between various salt concentration units in H4 and F4, including the mole fraction of salt, x_{salt}, weight percent salt, molality, and concentration in units of moles per cubic centimeter. The concentration of salt is denoted c, that of the solvent is denoted c_0, and the total concentration is $c_T = c_0 + 2c$, because each salt molecule contains two ions. The maximum concentrations studied were limited by the solubility limits.[52]

Experimental characterization.—All experiments were conducted at 30 °C. All error bars are standard deviations from at least three replicate measurements. In order to produce figure insets showing the ratio of properties in H4 and F4, linear interpolation was used to estimate the properties at the same salt concentrations in the two systems. Therefore, these insets should be regarded as approximations.

Conductivity measurements.—Ionic conductivity, denoted κ, of H4 and F4 was measured using a FiveEasy Conductivity Meter F30 (Mettler Toledo). Conductivity for the F4 system has been reported elsewhere.[52] Each measurement was carried out in triplicate.

Electrochemical characterization.—All other electrochemical techniques were performed as described by Shah et al.,[52] and all results are tabulated in Table SI. Current fraction, ρ_+, previously referred to as ideal transference number, $t_{+,id}$, was determined using polarization of lithium symmetric cells and Eq. 4,

$$\rho_+ = \frac{I_{ss}}{I_\Omega}\left(\frac{\Delta V - I_\Omega R_0}{\Delta V - I_{ss}R_{ss}}\right), \qquad [4]$$

where I_{ss} is the steady-state current, $I_\Omega = \Delta V/R_T$ where R_T is the total resistance measured by ac impedance spectroscopy, ΔV is the applied polarization potential, R_0 is the initial interfacial resistance, and R_{ss} is the interfacial resistance at steady-state.

Restricted diffusion coefficients were determined by measuring the open-circuit potential, U, of lithium symmetric cells after polarization.[20] The relaxation profiles were fit to Eq. 5,

$$U(t) = k_0 + ae^{-bt}, \qquad [5]$$

where k_0 is an empirical offset voltage and a and b are fit parameters. The salt diffusion coefficient within the separator, D_s, is then determined by Eq. 6,

Table I. Salt concentration in electrolytes.

	x_{salt}	wt% salt	molality (mol kg^{-1})	density (g l^{-1})	c $\times 10^3$ (mol cm^{-3})	$c_0 \times 10^3$ (mol cm^{-3})	$c_T \times 10^3$ (mol cm^{-3})
H4	0.04	5.0	0.18	990	0.17	4.2	4.6
	0.24	29.3	1.44	1240	1.27	3.9	6.5
	0.46	52.1	3.78	1440	2.57	3.1	8.2
	0.55	60.8	5.39	1490	3.15	2.6	8.9
F4	0.03	1.0	0.05	1490	0.08	2.8	2.9
	0.13	5.0	0.28	1450	0.39	2.6	3.4
	0.24	10.0	0.60	1660	0.89	2.8	4.6
	0.33	14.9	0.94	1680	1.36	2.7	5.4
	0.41	19.6	1.30	1630	1.70	2.5	5.9
	0.48	25.0	1.78	1760	2.36	2.5	7.2

$$D_s = \frac{l^2 b}{\pi^2}, \qquad [6]$$

where l is the thickness of the separator stack. Celgard 2500 separators (thickness 25 μm, diameter 19 mm) were soaked with the electrolyte. Three configurations were used for F4, with 5, 10, and 15 separators stacked to adjust the thickness of the electrolytes. Only one configuration was used for H4, with 20 separators stacked. The electrolyte diffusion coefficient, D, is then τD_s, where τ is the tortuosity of the separator ($\tau = 4.53 \pm 0.45$ as reported in Ref. 52).

The open-circuit potential was measured using concentration cells with a *U*-cell design to determine the thermodynamic factor using Eq. 7,

$$1 + \frac{\mathrm{d}\ln\gamma_{\pm}}{\mathrm{d}\ln m} = \frac{\kappa(z_+\nu_+)}{\nu RTDc\left(\frac{1}{\rho_+} - 1\right)}\left(\frac{\mathrm{d}U}{\mathrm{dln}m}\right)^2, \qquad [7]$$

where z_+ is the cation charge number, ν_+ is the number of cations, ν is related to the stoichiometric factor, and c is the salt concentration. For univalent salts, z_+ and ν_+ are 1, and ν is 2. The thermodynamic factor can be used to calculate the transference number of the electrolyte phase, t_+^0, according to Eq. 8,

$$t_+^0 = 1 - \sqrt{\frac{\frac{F^2Dc}{\nu\kappa RT}\left(\frac{1}{\rho_+} - 1\right)}{1 + \frac{\mathrm{d}\ln\gamma_{\pm}}{\mathrm{d}\ln m}}}. \qquad [8]$$

Viscosity.—Electrolyte viscosities were measured using an electromagnetically spinning viscometer (EMS-1000, Kyoto Instruments). Electrolytes were sealed in tubes in the glovebox, rendering the measurement air-free, and samples were maintained at 30 °C by the instrument. Bulk sample viscosity is determined from the rotation rate of an aluminum sphere within the solution as it is spun by an external applied magnetic field. No dependence on rotation rate was observed within instrument capabilities, and reported values were taken at a rate of 1,000 rpm. Error was estimated from at least 10 repeat measurements on the same sample.

Pulsed-field gradient NMR.—Self-diffusion coefficients were measured using pulsed-field gradient NMR (PFG-NMR).[57] NMR samples were prepared under Ar in 5 mm tubes with high-pressure caps. Measurements on F4 were performed on a 600 MHz Bruker Avance III instrument using a broadband observe Smart probe (BBO) with a Z-gradient (maximum gradient strength 50 G cm^{-1}) and a variable temperature unit maintained at 30 °C. Diffusion data for the H4 samples were acquired on the same instrument but with a broadband observe Prodigy cryo-probe (BBO) with a Z-gradient (maximum gradient strength 67 G cm^{-1}). Measurements were performed at 233.23 MHz for ^{7}Li, 565.63 MHz for ^{19}F, and 600.13 MHz for ^{1}H. For F4, ^{19}F NMR was used to measure the diffusion of both the anion and the polymer backbone. The peak at 50 ppm was assigned to the anion.[52] For H4, due to the lack of fluorination of the polymer, ^{1}H NMR was used to measure the diffusion of the polymer backbone.

For each nucleus at each salt concentration, inversion recovery experiments were used to measure T_1 relaxation constants in order to ensure that the recycle delay was maintained above 5 times T_1. T_1 data for all measured nuclei in both systems as a function of salt concentration are shown in Fig. S1 of the Supplemental Information (available online at stacks.iop.org/JES/167/120540/mmedia). For all H4 samples, and all F4 samples below $x_{salt} = 0.4$, data were acquired using a double stimulated echo sequence with bipolar gradients and convection compensation (Bruker pulse sequence dstebpgp3s). A stimulated echo sequence with bipolar gradients without convection correction (Bruker pulse sequence stebpgp1s) was used for F4 samples with $x_{salt} > 0.4$ due to low sensitivity. These samples have the highest viscosity (see Fig. 2c), so it is reasonable to expect that convection is less likely to be significant. If convection is a factor, one would expect that larger diffusion delay times, Δ, would result in faster observed diffusion coefficients. Therefore, when convection correction was not used, experiments were conducted with a variety of diffusion delays and pulse lengths to confirm that convection was not a source of error. For F4, diffusion delays, Δ, from 0.5 to 1 s (^{7}Li) and 0.07 to 0.15 s (^{19}F), and magnetic field gradient pulse lengths, δ, from 16 to 40 ms (^{7}Li) and 2 to 11 ms (^{19}F) were used. For H4, Δ from 0.4 to 1.6 s (^{7}Li), 0.3 to 1 s (^{19}F), and 0.3 to 1.1 s (^{1}H), and δ from 1.6 to 4.4 ms (^{7}Li), 1.2 to 3.4 ms (^{19}F), and 0.8 to 2.8 ms (^{1}H) were used.

For the convection-corrected experiments, the signal attenuation was fit to Eq. 9,[58]

$$E = e^{-\gamma^2 g^2 \delta^2 D_{\mathrm{self,i}}\left(\Delta - \frac{5\delta}{8} - \tau_d\right)}, \qquad [9]$$

where E is the signal attenuation, γ is the gyromagnetic ratio, g is the pulsed field gradient strength, $D_{\mathrm{self,i}}$ is the self-diffusion coefficient of species i, and τ_d is a delay for gradient recovery. For non-convection corrected experiments, E was fit to Eq. 10,[58]

$$E = e^{-\gamma^2 g^2 \delta^2 D_{\mathrm{self,i}}\left(\Delta - \frac{\delta}{4}\right)}. \qquad [10]$$

Both Eqs. 9 and 10 include corrections for sine-shaped gradient pulses.[58] For each diffusion measurement, 32 experiments with varying gradient strengths spaced linearly between 5% and 95% of the maximum

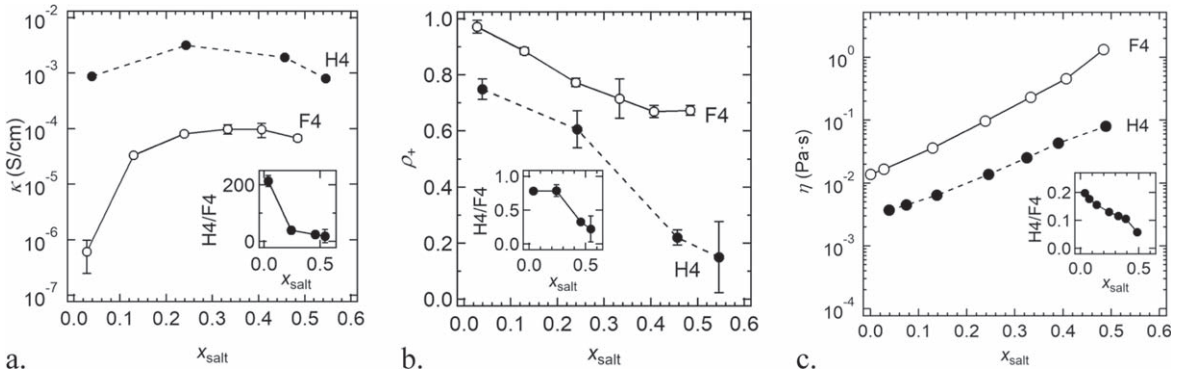

Figure 2. Ionic conductivity, κ (a), current fraction, ρ_+ (b), and viscosity, η (c) as a function of salt concentration, x_{salt}, for H4 and F4. Insets show the ratios of properties in H4 vs F4.

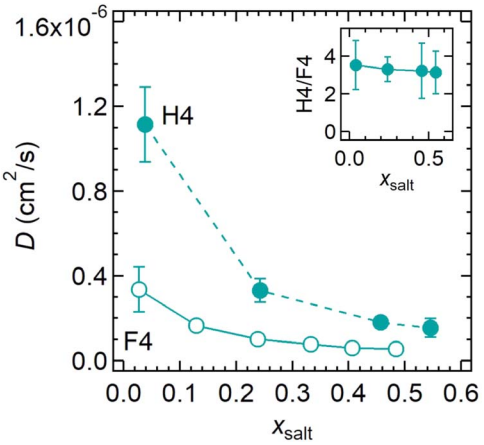

Figure 3. Salt diffusion coefficients, D, measured by the restricted diffusion technique. Inset shows the ratio of D in H4 vs F4.

gradient strength were performed, always resulting in linear signal attenuation on Stejskal-Tanner plots.[57] A representative Stejskal-Tanner plot is shown in Fig. S2 of the Supplemental Information.

Results and Discussion

Figure 2a shows the ionic conductivity of tetraglyme/LiTFSI (H4) and C8-DMC/LiFSI (F4) electrolytes as a function of salt mole fraction, x_{salt}. We chose to express salt concentration in terms of mole fraction rather than molality because the molar masses of the solvents differ substantially; Table I can be used to convert between concentration units. Both systems exhibit similar trends, with the conductivity increasing with concentration at low concentration and reaching a shallow maximum at moderate concentration ($x_{salt} = 0.24$ for H4 and 0.33 for F4) before decreasing at higher salt concentrations. However, the conductivity in H4 is one to two orders of magnitude higher than that of F4. In Fig. 2 (and in subsequent Figs. 3–5 and 7), we provide insets showing the ratio of the plotted parameters in H4 vs F4. The ratio of conductivities shown in the inset in Fig. 2a ranges from 210 at low salt concentration to 18 at high salt concentration. Our measured ionic conductivity for H4 is in excellent agreement with data in Refs. 26 and 29. Figure 2b shows the current fraction, ρ_+, measured by the Bruce-Vincent method.[50,51] ρ_+ decreases with salt concentration in both systems, but at all salt concentrations, ρ_+ is significantly higher in F4 than in H4. κ and ρ_+ data for F4 are adapted from Ref. 52 by permission of the PCCP Owner Societies. Figure 2c shows viscosity in both systems, and these results are also shown in Table SII. Despite the similar chain lengths in H4 and F4, the viscosities differ by approximately an order of magnitude, with F4 being significantly more viscous. At high salt concentrations, the viscosity of F4 is a factor of 17 higher than that of H4. Our measured viscosities agree well with those reported in Ref. 26 for H4.

It is tempting to try to determine which electrolyte is "better" for lithium ion transport based on the data in Fig. 2. If ionic conductivity were the only important parameter, then clearly H4 is the better electrolyte. However, in the limit of small dc currents, the efficacy of an electrolyte is given by the product $\kappa\rho_+$.[23,42,50,59,60] At high salt concentration in the vicinity of $x_{salt} = 0.5$, the conductivity of H4 is higher than that of F4 by about an order of magnitude, but ρ_+ of H4 is lower than that of F4 by about the same factor. Using $\kappa\rho_+$ to evaluate efficacy thus suggests that H4 and F4 are equally "good" electrolytes at high salt concentrations. Despite this observation, we expect the interactions between the ions and the solvent to be very different in H4 and F4. It is difficult, however, to determine what aspect of this difference affects κ and ρ_+. In the discussion below, we illustrate that complete characterization (beyond κ and ρ_+) is crucial for making inferences about lithium ion transport.

Figure 3 shows the salt diffusion coefficients, D, measured by the restricted diffusion method.[20] In both H4 and F4, D decreases

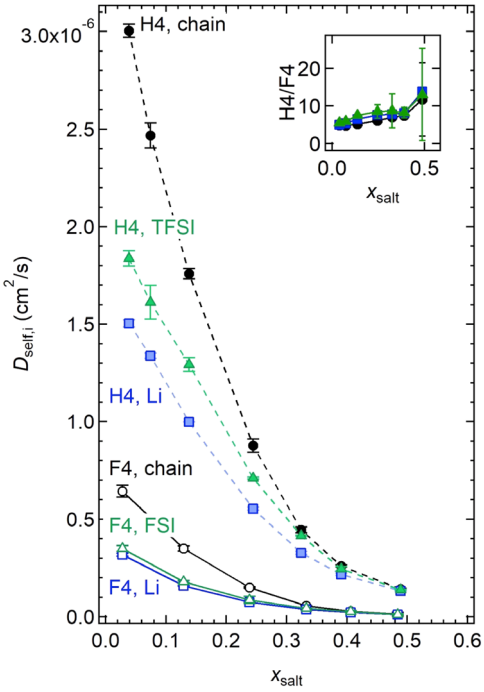

Figure 4. Self-diffusion coefficients of the cation (blue), anion (green), and polymeric solvent chain (black) in H4 (filled symbols) and in F4 (open symbols) as a function of salt concentration. The inset shows the ratio of the diffusivities in the two systems for the cation, anion, and chain.

exponentially with increasing salt concentration. At all salt concentrations, D is higher in H4 than in F4, consistent with the lower viscosity measured in H4. D data for F4 is adapted from Ref. 52 by permission of the PCCP Owner Societies.

Figure 4 shows the self-diffusion coefficients of the cation, anion, and polymeric solvent, $D_{self,+}$, $D_{self,-}$, and $D_{self,0}$, respectively, measured by PFG-NMR. $D_{self,+}$ and $D_{self,-}$ for F4 are adapted from Ref. 52 by permission of the PCCP Owner Societies. In simple mixtures of non-interacting, uncharged molecules, self-diffusion coefficients are inversely proportional to molar mass.[35] For both H4 and F4, however, the polymer diffusion coefficient was found to be higher than that of either cation or anion. The molar masses of the polymeric solvents are 222 and 526 g mol^{-1}, that of the anions, $TFSI^-$ and FSI^-, are 280 and 180 g mol^{-1} for H4 and F4, respectively, and that of Li^+ is 7 g mol^{-1}. It may therefore be surprising that the diffusivities of the solvents are so much higher than those of the ions. The trends observed in Fig. 4 are, however, consistent with data presented in Refs. 26 and 29 for H4. These results emphasize the importance of interactions between the ions and the polymer chains, as they cannot be explained without such interactions. In addition, the cation and anion self-diffusion coefficients are virtually identical in F4, while in H4, $D_{self,-}$ is higher than $D_{self,+}$. This suggests that the nature of ion-polymer and ion-ion interactions are different in the two systems.

The relationship between mutual and self-diffusion coefficients is often analyzed using the Nernst-Hartley relation, which gives a mutual diffusion coefficient in dilute electrolytes with dissociated salts.[61–64] However, the Nernst-Hartley relation does not include solvent diffusivity. We therefore define an analogous diffusion coefficient, D_{self}, which is similar in form to that defined by Nernst-Hartley but with the addition of a $D_{self,0}$ term:

$$\frac{1}{D_{self}} = \frac{x_0}{D_{self,0}} + \frac{x_+}{D_{self,+}} + \frac{x_-}{D_{self,-}}. \qquad [11]$$

D_{self}, along with D reproduced from Fig. 3 for comparison, is shown as a function of salt concentration in Fig. 5. As might be expected

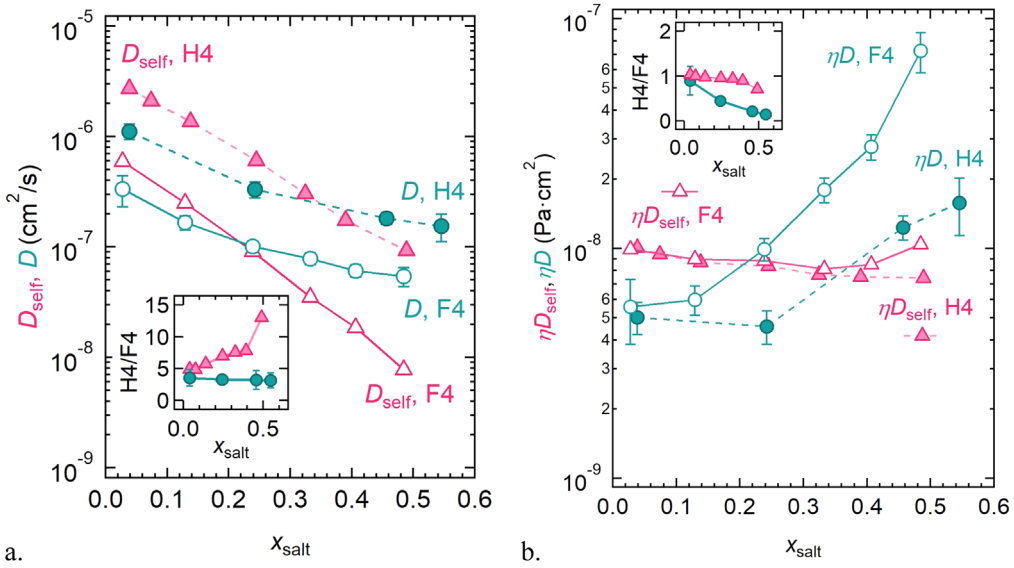

Figure 5. D_{self} (Eq. 11) (pink) and D (reproduced from Fig. 3 for comparison) (turquoise) (a), and D_{self} (pink) and D (turquoise) corrected by multiplication by viscosity (b) in H4 (filled symbols) and F4 (open symbols). Insets shows the ratio of D_{self} and D, and ηD_{self} and ηD, in H4 vs F4.

from the self-diffusion coefficient measurements (Fig. 4), D_{self} decreases exponentially with increasing salt concentration in both systems. In both systems, D_{self} is higher than D at low salt concentrations and lower than D at high salt concentrations. D_{self} of H4 is about an order of magnitude larger than that of F4 at all salt concentrations.

For simple systems, such as dilute colloidal spheres suspended in a solvent, diffusion and viscosity are related by the Stokes-Einstein relationship, and this implies that the product ηD should be a constant.[65,66] In Fig. 5b, we plot the product ηD_{self} as a function of salt concentration, and observe remarkable agreement between the two systems. This product is approximately 10^{-8} Pa · cm^2, and independent of salt concentration and the molecular structures of the anion and polymer. Figure 5b also shows the product ηD as a function of salt concentration. While the viscosity-corrected diffusion (ηD) values agree well between H4 and F4 at low salt concentrations, they diverge at higher salt concentrations. For neither system is the product ηD independent of salt concentration. It is clear that viscosity does not explain the dependence of D on salt concentration. Viscosity certainly affects ion transport, but more complex interactions must also come into play.

The conductivity and self-diffusion coefficient data in Figs. 2a and 4 enable calculation of β_{self} using Eq. 1. The results thus obtained for H4 and F4 are shown in Fig. 6. If our electrolytes were thermodynamically ideal, which one might expect to be the case in the dilute limit, then β_{self} would approach unity in the limit $x_{salt} \to 0$. In H4 and F4, deviations from thermodynamic ideality are evident, even in the most dilute electrolytes we study. The qualitative dependence of β_{self} on x_{salt} is different in the two systems, with of β_{self} in F4 increasing monotonically to its highest value ($\beta_{self} = 0.35$) at its highest salt concentration, while β_{self} in H4 reaches a maximum ($\beta_{self} = 0.61$) at intermediate salt concentration ($x_{salt} = 0.46$). The data for H4 agree with reported data in Refs. 26 and 29; however, these references only study salt concentrations below $x_{salt} = 0.5$, and therefore observe a monotonic increase in β_{self}. F4 could not be studied at higher salt concentrations due to its solubility limit.[52] β_{self} values in H4 and F4 are also quantitatively different, particularly at low salt concentration; the lowest β_{self} in F4 is 0.003, and in H4 the minimum is 0.42. This difference is obtained despite the similarity of the dependence of ion self-diffusion coefficients and conductivity on x_{salt}.

β_{self} is often called ionicity, and it is often argued to be a measure of the extent of dissociation of the salt ions because empirically-derived values are often less than unity.[26–29,33,38–41] This argument

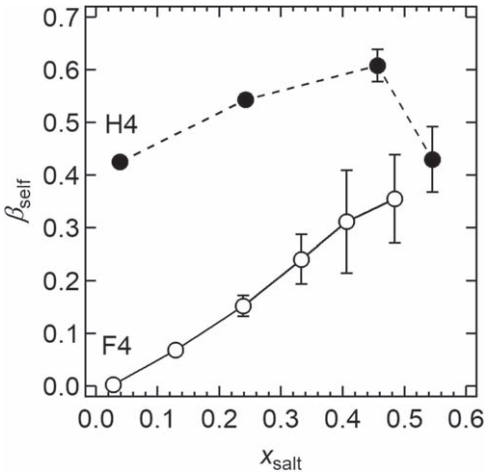

Figure 6. Pre-factor β_{self} relating conductivity to self-diffusion coefficients of the ions (Eq. 1) as a function of salt concentration for H4 (filled symbols) and F4 (open symbols).

rests on the assumption that lower-than-expected values of conductivity are obtained because only a fraction of ions present in the system are free to migrate under applied potentials with mobilities that are controlled by self-diffusion coefficients according to the Nernst equation; when β_{self} is low, many ions are assumed to be in neutral ion pairs. Since ion pairing and clustering increases with increasing salt concentration, we would expect β_{self} to decrease with increasing salt concentration. This is clearly not the case in F4, implying that in this system, β_{self} has little to do with the extent of dissociation. In other words, ionic conductivity is unrelated to self-diffusion in F4. The decrease of β_{self} between the two highest salt concentrations in H4 may, in principle, be related to ion pairing, but more evidence is required to establish if this explanation is correct. It is clear, however, that the polymer-ion interactions and charge transport mechanisms must be different in the two systems.

The factors that determine the conductivity and the interactions between ions is not clear from the data in Figs. 2–6. We sought to resolve this by performing additional electrochemical characterization experiments. In addition to frictional interactions, ion transport depends on thermodynamic effects that are quantified by the chemical potential of the salt. The thermodynamic contribution to ion transport, often referred to as the thermodynamic factor, is

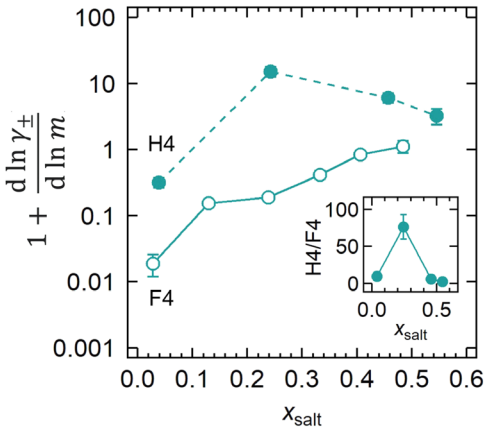

Figure 7. Thermodynamic factor in H4 (filled symbols) and F4 (open symbols). Inset shows the ratio of the thermodynamic factors in H4 vs F4.

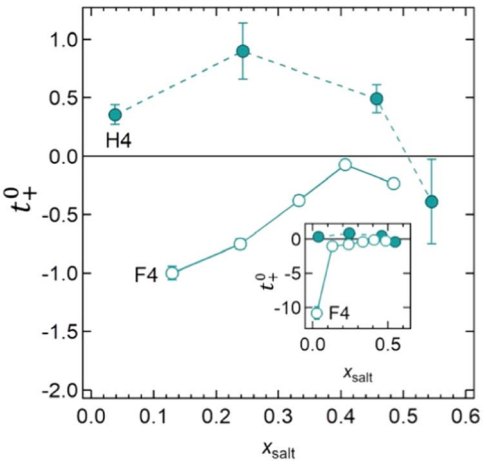

Figure 8. Rigorously-defined transference number, t_+^0 in H4 (filled symbols) and F4 (open symbols). The inset includes the data at the lowest salt concentration for F4.

determined by the dependence of the mean molal activity coefficient of the salt, $\gamma_\pm$, on salt concentration (molality), and is given by $1 + \frac{d \ln \gamma_\pm}{d \ln m}$.[19] Figure 7 shows the dependence of the thermodynamic factor on salt concentration for H4 and F4. The data for F4 are adapted from Ref. 52 by permission of the PCCP Owner Societies. In F4, the thermodynamic factor increases monotonically with salt concentration. In H4, the thermodynamic factor is a non-monotonic function of salt concentration, reaching a maximum at $x_{salt} = 0.24$. It is higher than that of F4 by one to two orders of magnitude.

The salt mutual diffusion coefficient plotted in Fig. 3 is related to the thermodynamic factor as shown in Eq. 12,

$$D = \mathfrak{D}\frac{c_T}{c_0}\left(1 + \frac{d \ln \gamma_\pm}{d \ln m}\right), \qquad [12]$$

where $\mathfrak{D}$ is the salt diffusion coefficient based on a thermodynamic driving force.

The thermodynamic factor, combined with measurements of κ, ρ_+, and D, can be used to calculate the transference number, t_+^0, using Eq. 8. The results are shown in Fig. 8, where t_+^0 is plotted as a function of x_{salt}. t_+^0 for F4 is adapted from Ref. 52 by permission of the PCCP Owner Societies. For F4, the transference number is negative at all salt concentrations. It increases with salt concentration, reaching a maximum of -0.07 at $x_{salt} = 0.41$. At the lowest salt concentration, $x_{salt} = 0.41$, shown only in the inset for ease of comparison of other salt concentrations, t_+^0 is -10.8. However, in H4, the transference number is positive at low and moderate salt concentrations, reaching a maximum of 0.90 at $x_{salt} = 0.24$, but then becomes negative at $x_{salt} = 0.55$. We note that this is a very different trend from that seen in ρ_+ (compare Figs. 8 and 2b). At all concentrations, ρ_+ of F4 is higher than that of H4. The opposite is true for t_+^0. It should be evident that ρ_+ is not a good approximation for the transference number in either H4 or F4.

The overall diffusion coefficient based on a thermodynamic driving force, $\mathfrak{D}$, depends on frictional interactions between all of the species in solution, and can be calculated using Eq. 12 and the data in Figs. 3 and 7. The ion-solvent and ion-ion frictional interactions are quantified by Stefan-Maxwell diffusion coefficients, $\mathfrak{D}_{0+}$, $\mathfrak{D}_{0-}$, and $\mathfrak{D}_{+-}$. Concentrated solution theory relates these diffusion coefficients to ion transport parameters introduced above[19]:

$$\mathfrak{D}_{0+} = \frac{-z_-}{z_+ - z_-}\frac{\mathfrak{D}}{1 - t_+^0}, \qquad [13]$$

$$\mathfrak{D}_{0-} = \frac{z_+}{z_+ - z_-}\frac{\mathfrak{D}}{t_+^0}, \qquad [14]$$

$$\text{and } \mathfrak{D}_{+-} = \left(\frac{-z_+ z_- c_T F^2}{\kappa RT} - \frac{z_+ - z_-}{z_+ \nu_+}\frac{c_0 t_+^0 (1 - t_+^0)}{c\mathfrak{D}}\right)^{-1}. \qquad [15]$$

$\mathfrak{D}_{0-}$ characterizes interactions between the polymer and the anion, $\mathfrak{D}_{0+}$ between the polymer and the cation, and $\mathfrak{D}_{+-}$ between the cation and the anion. All of the parameters on the right sides of Eqs.13–15 have been measured as a function of salt concentration. This enables calculation of the Stefan-Maxwell diffusion coefficients.

In Fig. 9a, we plot $\mathfrak{D}_{0+}$ as a function of salt concentration. The inset shows the same data with a different y-axis scale for visibility of small diffusion coefficients. At low salt concentrations, $\mathfrak{D}_{0+}$ is significantly higher in H4 than in F4. At $x_{salt} = 0.24$ and above, $\mathfrak{D}_{0+}$ in H4 and F4 are very similar to each other. Given the fact that the self-diffusion coefficients of the lithium ions in H4 and F4 are very different at all salt concentrations, this agreement is perhaps surprising. This suggests that despite differences in apparent ion transport behavior, at moderate to high salt concentrations, the frictional interactions between the lithium cation and the polymer are similar in both fluorinated and non-fluorinated systems. This similarity can only be observed after thermodynamic effects have been properly accounted for using the concentrated solution theory approach.

In Fig. 9b and its inset, we plot $\mathfrak{D}_{0-}$ as a function of salt concentration. Here we see dramatic differences between H4 and F4, indicating differences in the frictional interactions between the anion and polymer. In H4, as with $\mathfrak{D}_{0+}$, $\mathfrak{D}_{0-}$ is large and positive at low salt concentrations, then decreases rapidly, but unlike $\mathfrak{D}_{0+}$, $\mathfrak{D}_{0-}$ becomes slightly negative at $x_{salt} = 0.55$. The behavior seen in F4 is yet more complex: $\mathfrak{D}_{0-}$ is negative at all salt concentrations, but the magnitude decreases with increasing salt concentration. This complexity supports the hypothesis that one of the main differences between H4 and F4 is the presence of the fluorous effect in F4, which influences interactions between the fluorinated anion and the fluorinated chain. This is consistent with other recent studies on fluorinated ether-based electrolytes.[12]

Equation 3 indicates that t_+^0 depends only on $\mathfrak{D}_{0+}$ and $\mathfrak{D}_{0-}$. Because $\mathfrak{D}_{0+}$ of H4 and F4 are in good agreement at high salt concentrations, we conclude that the difference in t_+^0 observed in this regime in Fig. 8 must be due to differences in anion interactions with the backbone which are captured in $\mathfrak{D}_{0-}$. At low salt concentrations, neither $\mathfrak{D}_{0-}$ nor $\mathfrak{D}_{0+}$ agrees between the two systems, so differences in both cation-solvent and anion-solvent interactions are responsible for the difference in transference number.

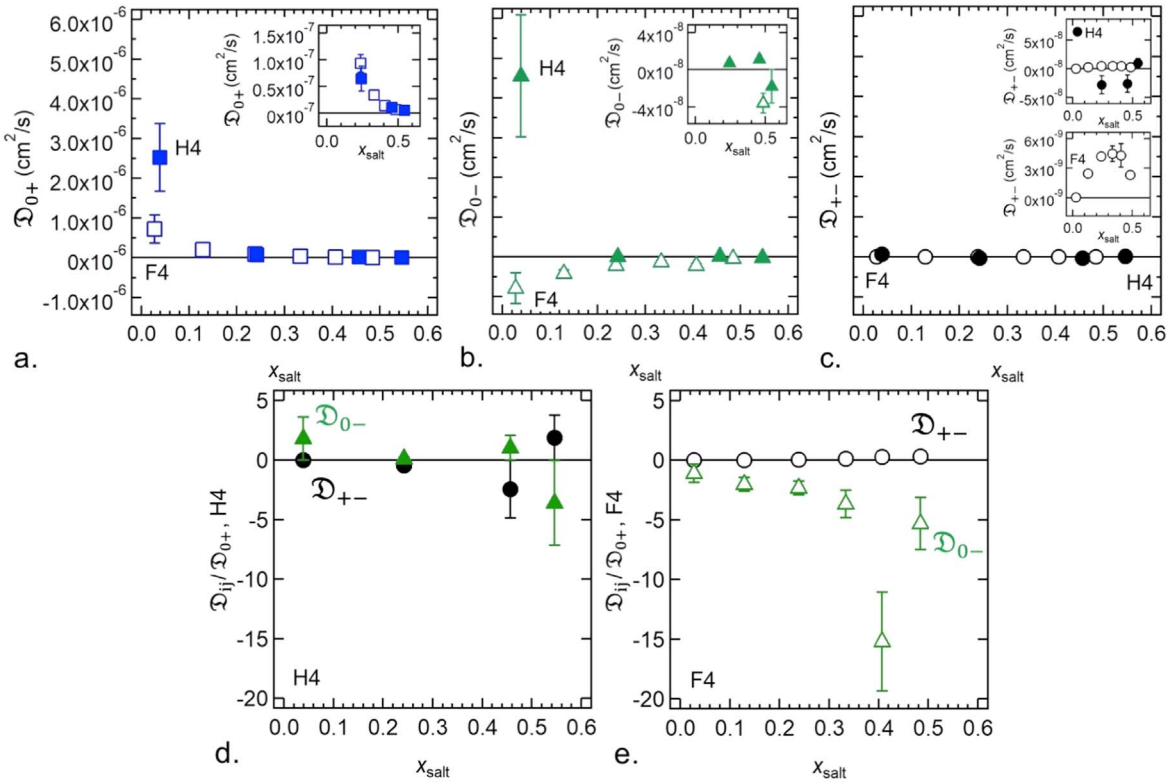

Figure 9. Stefan-Maxwell diffusion coefficients $\mathfrak{D}_{0+}$ (a), $\mathfrak{D}_{0-}$ (b), and $\mathfrak{D}_{+-}$ (c) calculated for H4 (filled symbols) and F4 (open symbols) as a function of salt concentration. Insets show the same data expanded for small values of $\mathfrak{D}$. The ratio of $\mathfrak{D}_{0-}$ (green) and $\mathfrak{D}_{+-}$ (black) to $\mathfrak{D}_{0+}$ for H4 (d) and F4 (e).

In Fig. 9c and its insets, we plot $\mathfrak{D}_{+-}$ as a function of salt concentration. In Figs. 9d and 9e, we plot the ratios of $\mathfrak{D}_{0-}$ and $\mathfrak{D}_{+-}$ to $\mathfrak{D}_{0+}$ for H4 and F4, respectively. In both H4 and F4, $\mathfrak{D}_{+-}$ is very small relative to $\mathfrak{D}_{0+}$. In F4, it is also small relative to $\mathfrak{D}_{0-}$, while in H4, $\mathfrak{D}_{+-}$ and $\mathfrak{D}_{0-}$ are similar in magnitude at high salt concentrations. In F4, $\mathfrak{D}_{+-}$ is positive at all salt concentrations, reaching a shallow maximum at intermediate salt concentrations. In H4, it is relatively large and positive at low salt concentration, then fluctuates between positive and negative at higher salt concentrations. $\mathfrak{D}_{+-}$ characterizes cation-anion interactions and is ignored in dilute solution theory due to the assumption of fully-dissociated ions. The inverse of $\mathfrak{D}_{+-}$ describes friction between the ions, so a small $\mathfrak{D}_{+-}$ indicates that there is a large amount of friction between cation and anion and that the assumption of full dissociation is likely to be invalid. The motion of cations in electrolytes depends on $\mathfrak{D}_{0+}$ and $\mathfrak{D}_{+-}$, while the motion of anions depends on $\mathfrak{D}_{0-}$ and $\mathfrak{D}_{+-}$. The smaller of the two diffusion coefficients dominates, and so we expect $\mathfrak{D}_{+-}$ to be important in both H4 and F4 due to its small magnitude. Thus, the data in Fig. 9 indicate that concentrated solution theory is necessary to understand ion transport in both systems.

We can use concentrated solution theory to elucidate the underpinnings of the vastly different conductivities reported in Fig. 2a. Concentrated solution theory provides an equation relating the ionic conductivity to the Stefan-Maxwell diffusion coefficients:[19]

$$\frac{1}{\kappa} = \frac{-RT}{c_T z_+ z_- F^2}\left(\frac{1}{\mathfrak{D}_{+-}} - \frac{c_0 z_-}{\nu_+ c(z_+\mathfrak{D}_{0+} - z_-\mathfrak{D}_{0-})}\right). \quad [16]$$

Equation 16 illustrates that conductivity is given by the addition of two diffusive contributions, one related to the frictional interactions between the cation and anion, and the other related to frictional interactions between the ions and the solvent. It is conceivable that in some systems, one of these contributions is dominant.

If the frictional interactions between ions are dominant, we can re-express Eq. 16 in a form that is reminiscent of the Nernst-Einstein equation (Eq. 1):

$$\kappa = -\beta_{+-}\frac{c_T z_+ z_- F^2}{RT}(\mathfrak{D}_{+-}). \quad [17]$$

We have introduced a pre-factor, β_{+-}, in Eq. 17 to account for the fact that the relationship between κ and $\mathfrak{D}_{+-}$ is obtained by ignoring frictional interactions between the ions and the solvent and is therefore certainly not expected to apply universally. β_{+-} is similar in spirit to β_{self} in the Nernst-Einstein equation. If the experimentally-determined values of κ and $\mathfrak{D}_{+-}$ are such that β_{+-} is in the vicinity of unity, then we would infer that in such a system, frictional interactions between the ions and the solvent can be ignored.

Correspondingly, if ion-solvent interactions are dominant, then we can re-express Eq. 16 as

$$\kappa = \beta_0\frac{F^2 c c_T}{RTc_0}(z_+^2\nu_+\mathfrak{D}_{0+} + z_-^2\nu_-\mathfrak{D}_{0-}), \quad [18]$$

where we have introduced a pre-factor, β_0, that is similar to β_{+-} and β_{self}. If the experimentally-determined values of κ, $\mathfrak{D}_{0+}$, and $\mathfrak{D}_{0-}$ are such that β_0 is in the vicinity of unity, then we would infer that in such a system, frictional interactions between the cation and anion can be ignored.

In the dilute limit, we can write

$$\frac{c_T\nu_+ c}{c_0} = \frac{(c_0 + \nu_+ c + \nu_- c)\nu_+ c}{c_0} = \frac{c_0\nu_+ c}{c_0} = \nu_+ c \quad [19]$$

because $c \ll c_0$. In this limit, Eq. 18 reduces to

$$\kappa = \beta_{0,c}\frac{cF^2}{RT}(z_+^2\nu_+\mathfrak{D}_{0+} + z_-^2\nu_-\mathfrak{D}_{0-}), \quad [20]$$

where we have introduced a pre-factor, $\beta_{0,c}$, that is similar to β_0. This dilute-limit approximation leaves Eq. 17 unchanged, so there is

no analogous $\beta_{+-,c}$. Equation 20 is identical to Eq. 1, the Nernst-Einstein equation, except that self-diffusion coefficients have been replaced by Stefan-Maxwell diffusion coefficients.

For a univalent salt such as LiTFSI or LiFSI, used here, where $z_+ = 1$, $z_- = -1$, and $\nu_+ = \nu_- = 1$, Eqs. 17, 18, 20, and 1 reduce to

$$\kappa = \beta_{+-}\frac{c_T F^2}{RT}(\mathfrak{D}_{+-}), \quad [21]$$

$$\kappa = \beta_0 \frac{F^2 c c_T}{RT c_0}(\mathfrak{D}_{0+} + \mathfrak{D}_{0-}), \quad [22]$$

$$\kappa = \beta_{0,c}\frac{cF^2}{RT}(\mathfrak{D}_{0+} + \mathfrak{D}_{0-}), \quad [23]$$

$$\text{and } \kappa = \beta_{self}\frac{cF^2}{RT}(D_{self,+} + D_{self,-}). \quad [24]$$

The set of equations above are Nernst-Einstein-like equations. In many respects, Eqs. 21 and 24 represent approximations at two ends of a spectrum. In a classical dilute electrolyte, wherein the motion of the cations and anions are entirely decoupled, i.e., the solution is thermodynamically ideal, one obtains Eq. 24. If, on the other hand, coulombic interactions between the cations and anions dominate, one obtains Eq. 21.

It is illustrative to examine the concentration-dependence of the newly-introduced β pre-factors in Eqs. 21–24 for a classical electrolyte. For KCl in water, we obtained values of κ from Ref. 67, and values of $\mathfrak{D}_{0+}$, $\mathfrak{D}_{0-}$, and $\mathfrak{D}_{+-}$ from Ref. 19. Figure 10 shows calculated values of β_{+-}, β_0, and $\beta_{0,c}$ thus obtained; we were unable to find literature data for D_{self} in KCl/water solutions, and so were unable to calculate β_{self}. In simple electrolytes with dissociated ions, one expects conductivity to be dominated by frictional interactions between the ions and the solvent. In this case, we expect β_0 and $\beta_{0,c}$ to be close to unity. In Fig. 10, at low salt concentrations, we see that this is true. At $x_{salt} = 0.002$, β_0 and $\beta_{0,c}$ are both 1.0 and $\beta_{+-} = 0.19$,, consistent with the expectation that, in dilute systems, cation-anion interactions are insignificant relative to ion-solvent interactions. As salt concentration increases, β_{+-} increases, indicating the increased contributions of cation-anion interactions to conductivity. At $x_{salt} = 0.07$, β_0 is 0.75, while β_{+-} is 0.44. This implies that frictional interactions between the ions and the solvent remain somewhat more important than cation-anion interactions even at this high salt concentration. We attach no significance to the observation that $\beta_{0,c}$ at high salt concentrations is closer to one than β_0. $\beta_{0,c}$ is necessarily greater than β_0 because c_T/c_0 is always greater than or equal to one (Eq. 19).

Figure 11a shows the β pre-factors from Eqs. 21–24 in H4. In addition to β_{+-}, β_0, and $\beta_{0,c}$, we have included β_{self} data from Fig. 6. For H4 at the lowest salt concentration, $x_{salt} = 0.04$, we find that $\beta_{self} = 0.27$, $\beta_0 = 0.19$, $\beta_{0,c} = 0.20$, and $\beta_{+-} = 0.81$. These values are qualitatively different from those obtained in KCl/water, with β_{+-} being closest to one, indicating that cation-anion interactions are more significant than ion-solvent interactions, even at very low salt concentrations. At higher salt concentrations, the magnitudes of all of the β pre-factors other than β_{self} are large relative to unity. These values indicate that all of the binary interactions in solution affect conductivity, and that neglecting any one of them cannot be justified. These observations also show that conclusions regarding ionicity based on β_{self} in H4 are erroneous. The behavior of β_{+-}, β_0, and $\beta_{0,c}$ indicate that the system cannot be thought of as having 20%-40% dissociated ions diffusing freely with the remainder in neutral ion pairs; instead, there are complex interactions between ions and solvent and between cations and anions.

Figure 11b shows the β pre-factors from Eqs. 21–24 in F4. Note the differences in y-axis scales used in Figs. 11a and 11b. It is evident that β_{+-} for F4 is unity and β_0 and $\beta_{0,c}$ are nearly zero at all salt concentrations. This implies that conductivity in F4 over the entire salt concentration range is dominated by frictional interactions between the anion and the cation. Conversely, it implies that frictional interactions between the ions and the solvent do not affect conductivity. A possible explanation is that the salt ions in F4 are present in clusters, consistent with the expectation of a lower dielectric constant of F4,[54] and ion transport occurs mainly within the clusters. For appreciable conductivity, these clusters must exhibit a percolating morphology. We note that this is consistent with the self-diffusion trends observed in Fig. 4; if the ions form a network-like percolating morphology, then it is unsurprising that they diffuse slowly relative to the polymeric solvent, which is not part of this network. H4 is similar to a more traditional electrolyte, wherein ions are coordinated with the ether oxygens on the polymeric solvent, as evidenced by β_0 being non-zero. At low salt concentrations, a significant fraction of solvent molecules are uncoordinated and diffuse freely, leading to the trends observed in Fig. 4. It is clear that F4 is very different from a traditional electrolyte, and in this case also that β_{self} has little to do with ionicity. For example, at $x_{salt} = 0.48$, β_{self} is 0.35. It would be incorrect to conclude from this that 35% of the Li^+ and FSI^- ions are in a dissociated state in F4. In fact, the values of β_{+-} indicate that most, if not all, of the Li^+ and FSI^- ions are in clusters.

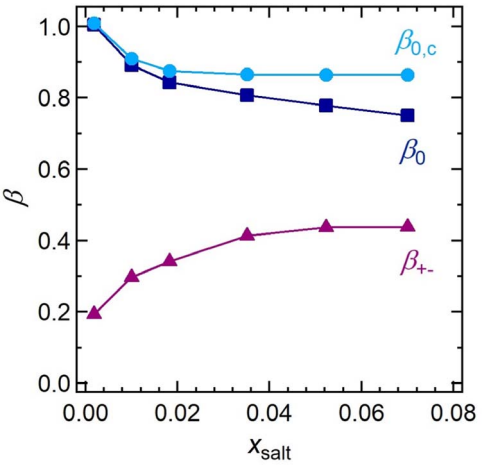

Figure 10. β_{+-} (purple), β_0 (dark blue), and $\beta_{0,c}$ (light blue) pre-factors in Eqs. 21–23 for KCl in water as a function of salt concentration.

Conclusions

We have used a variety of characterization techniques, including viscosity measurement, pulsed-field gradient NMR, and full electrochemical characterization, to study electrolytes made from tetraglyme mixed with LiTFSI (H4) and a fluorinated tetraglyme analog, C8-DMC, mixed with LiFSI (F4). We observe significant differences in properties, including conductivity, viscosity, and self-diffusion coefficients differing by one to two orders of magnitude, and differences in sign in the rigorously-defined transference number, t_+^0.

It is common in the literature, though not universal,[12,43,52] to focus on frictional interactions between the cation and the solvent to explain trends in the cation transference number. By analyzing our data using Newman's concentrated solution theory, we determine that at high salt concentrations, the differences in t_+^0 are due to differences in $\mathfrak{D}_{0-}$, which characterizes frictional interactions between the anion and the solvent chain. This can be explained by the fact that, due to the fluorous effect, the fluorinated backbone in F4 is expected to have much stronger interactions with a fluorinated anion than tetraglyme would be expected to have.

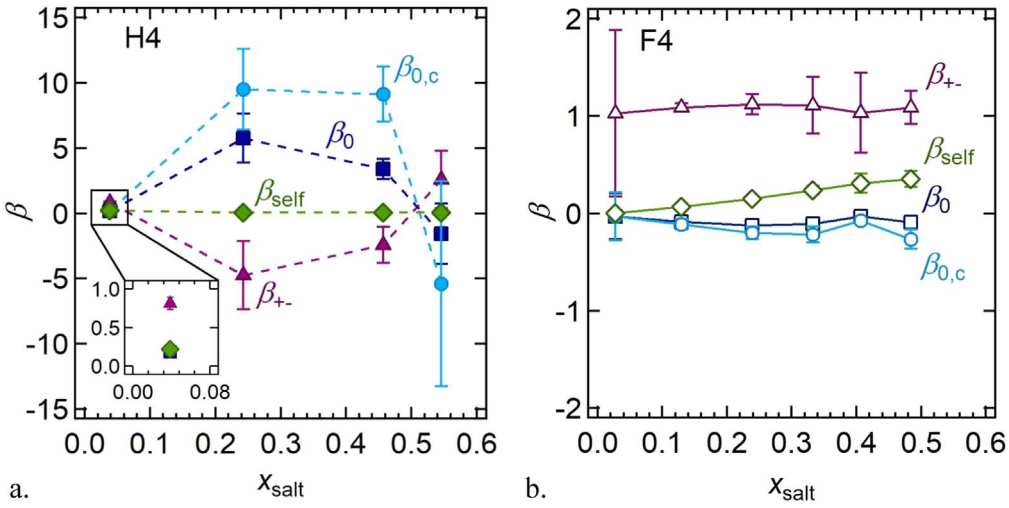

Figure 11. β_{+-} (purple), β_0 (dark blue), $\beta_{0,c}$ (light blue), and β_{self} (green) pre-factors from Eqs. 21–24 for H4 (a) and F4 (b) as a function of salt concentration. Inset of (a) shows the β pre-factors at $x_{salt} = 0.04$, with β_{self}, β_0, and $\beta_{0,c}$ all overlapping near $\beta = 0.2$.

Establishing the underpinnings of ionic conductivity was a major goal of this paper. It is common in the literature to assume that differences in conductivity arise due to differences in viscosity and self-diffusion coefficients of the ions. Quantitative differences between conductivity and self-diffusion are usually interpreted in terms of ionicity and quantified by the measured Nernst-Einstein pre-factor, β_{self}. It is therefore important to answer the three questions presented in the Introduction:

(1) Are differences in conductivity in H4 and F4 related to differences in ion self-diffusion coefficients, $D_{self,+}$ and $D_{self,-}$, as anticipated by Eq. 1?
(2) Are differences in conductivity in H4 and F4 related to differences in viscosity?
(3) Is β_{self} a measure of the extent of ion dissociation in H4 and F4?

The data presented in Figs. 7–11 indicate that the answers to all three questions is "no." In both H4 and F4, ionic conductivity is not dominated by frictional interactions between individual ions and the solvent and thus it is not related to the self-diffusion coefficients of the ions. The self-diffusion coefficients themselves are greatly affected by viscosity but conductivity is not. In both H4 and F4, it is incorrect to consider the electrolytes to be a simple mixture of free ions and ion pairs, indicating that the measured β_{self} has little to do with ionicity.

Using Newman's concentrated solution theory, we define pre-factors that are similar in spirit to the Nernst-Einstein pre-factor, β_{self}. The newly-defined pre-factors, however, acknowledge that conductivity is controlled by three independent frictional interactions: cation-solvent, anion-solvent, and cation-anion, which are quantified using Stefan-Maxwell diffusion coefficients. The simplest situation arises when conductivity is only dependent on frictional interactions between the ions and the solvent, which is the basis of Eq. 22 and the pre-factor β_0. To illustrate this situation, we sought an electrolyte in which the answers to the three aforementioned questions would be "yes," and in which Stefan-Maxwell diffusion coefficients had been measured. To our knowledge, however, no such electrolyte has been fully characterized. For the classical electrolyte aqueous KCl, we were unable to find measurements of ion self-diffusivities in the literature. Based on Stefan-Maxwell diffusion coefficients, however, we were able to show that the conductivity in this system can be understood in terms of β_0 in the dilute limit; β_0 is unity in the limit of low salt concentration, and decreases monotonically to a value of 0.75 at $x_{salt} = 0.07$. In contrast, the conductivity of F4 electrolytes is controlled by frictional interactions between the cation and the anion. We present Eq. 21 to describe ion transport in such systems, introducing a new pre-factor, β_{+-}. A remarkable observation is that β_{+-} in F4 is approximately equal to unity at all salt concentrations ($x_{salt} = 0.03$ to 0.48). We posit that such electrolytes contain transient clusters of ions and high conductivity is obtained only when the clusters form a percolating network-like structure.

Acknowledgments

This work was intellectually led by the Joint Center for Energy Storage Research (JCESR), an Energy Innovation Hub funded by the U.S. Department of Energy (DOE), Office of Science, Basic Energy sciences (BES), under Contract No. DEAC02-06CH11357. Electrolyte synthesis and characterization work was performed by L. S. G., D. B. S., and H. Q. N. under the supervision of N. P. B.; L. S. G. under the supervision of H. C.; and K. M. D. under the supervision of B. D. M. We thank UC Berkeley's NMR facility in the College of Chemistry (CoC-NMR) for spectroscopic assistance. Instruments in the CoC-NMR are supported in part by NIH S10OD024998. Electrolyte synthesis work was initially established by Kevin R. Olson, Sue J. Mecham, and J. M. D., who were supported by the Center for Mesoscale Transport Properties, an Energy Frontier Research Center supported by the U.S. Department of Energy, Office of Science, Basic Energy Sciences, under award #DE-SC0012673. The work of K. M. D. and B. D. M. was supported by the Assistant Secretary for Energy Efficiency and Renewable Energy, Office of Vehicle Technologies of the U.S. Department of Energy under Contract DE-AC02-05CH11231 under the Advanced Battery Materials Research (BMR) Program.

ORCID

Lorena S. Grundy https://orcid.org/0000-0001-7706-2216
Deep B. Shah https://orcid.org/0000-0001-7816-031X
Kyle M. Diederichsen https://orcid.org/0000-0002-6787-7996
Bryan D. McCloskey https://orcid.org/0000-0001-6599-2336
Nitash P. Balsara https://orcid.org/0000-0002-0106-5565

References

1. D. Aurbach, "Review of selected electrode solution interactions which determine the performance of Li and Li-ion Batteries." *J. Power Sources*, **89**, 206 (2000).
2. D. Aurbach, B. Markovsky, A. Shechter, Y. Ein-Eli, and H. Cohen, "A comparative study of synthetic graphite and li electrodes in electrolyte solutions based on ethylene carbonate-dimethyl carbonate mixtures." *J. Electrochem. Soc.*, **143**, 3809 (1996).

3. K. Xu, "Nonaqueous liquid electrolytes for lithium-based rechargeable batteries." *Chem. Rev.*, **104**, 4303 (2004).
4. E. R. Logan, K. L. Gering, X. Ma, and J. R. Dahn, "Electrolyte development for high-performance li-ion cells: additives, solvents, and agreement with a generalized molecular model." *Electrochem. Soc. Interface*, **28**, 49 (2019).
5. F. Ding et al., "Effects of carbonate solvents and lithium salts on morphology and coulombic efficiency of lithium electrode." *J. Electrochem. Soc.*, **160**, A1894 (2013).
6. A. Manthiram, "A reflection on lithium-ion battery cathode chemistry." *Nat. Commun.*, **11**, 1550 (2020).
7. M. Marzantowicz, J. R. Dygas, F. Krok, J. L. Nowiński, A. Tomaszewska, Z. Florjańczyk, and E. Zygadło-Monikowzka, "Crystalline phases, morphology and conductivity of PEO:LiTFSI electrolytes in the eutectic region." *J. Power Sources*, **159**, 420 (2006).
8. K. Murata, S. Izuchi, and Y. Yoshihisa, "An overview of the research and development of solid polymer electrolyte batteries." *Electrochim. Acta*, **45**, 1501 (2000).
9. D. T. Hallinan and N. P. Balsara, "Polymer electrolytes." *Annu. Rev. Mater. Res.*, **43**, 503 (2013).
10. X. Ren et al., "High-concentration ether electrolytes for stable high-voltage lithium metal batteries." *ACS Energy Lett.*, **4**, 896 (2019).
11. D. H. C. Wong, J. L. Thelen, Y. Fu, D. Devaux, A. A. Pandya, V. S. Battaglia, N. P. Balsara, and J. M. DeSimone, "Nonflammable perfluoropolyether-based electrolytes for lithium batteries." *PNAS*, **111**, 3327 (2014).
12. C. V. Amanchukwu, Z. Yu, X. Kong, J. Qin, Y. Cui, and Z. Bao, "A new class of ionically conducting fluorinated ether electrolytes with high electrochemical stability." *J. Am. Chem. Soc.*, **142**, 7393 (2020).
13. X. Fan et al., "Non-flammable electrolyte enables Li-metal batteries with aggressive cathode chemistries." *Nat. Nanotechnol.*, **13**, 715 (2018).
14. Y.-M. Lin, K. C. Klavetter, P. R. Abel, N. C. Davy, J. L. Snider, A. Heller, and C. B. Mullins, "High performance silicon nanoparticle anode in fluoroethylene carbonate-based electrolyte for Li-ion batteries." *Chem. Commun.*, **48**, 7268 (2012).
15. T. Hou, G. Yang, N. N. Rajput, J. Self, S.-W. Park, J. Nanda, and K. A. Persson, "The Influence of FEC on the solvation structure and reduction reaction of LiPF6/EC electrolytes and its implication for solid electrolyte interphase formation." *Nano Energy*, **64**, 103881 (2019).
16. R. Berger, G. Resnati, P. Metrangolo, E. Weber, and J. Hulliger, "Organic fluorine compounds: a great opportunity for enhanced materials properties." *Chem. Soc. Rev.*, **40**, 3496 (2011).
17. J. Self, K. D. Fong, E. R. Logan, and K. A. Persson, "Ion association constants for lithium ion battery electrolytes from first-principles quantum chemistry." *J. Electrochem. Soc.*, **166**, A3554 (2019).
18. K.-H. Shen and L. M. Hall, "Ion conductivity and correlations in model salt-doped polymers: effects of interaction strength and concentration." *Macromolecules*, **53**, 3655 (2020).
19. J. Newman and K. E. Thomas-Alyea, *Electrochemical Systems* (Wiley, New Jersey) (2004).
20. Y. Ma et al., "The measurement of a complete set of transport properties for a concentrated solid polymer electrolyte solution." *J. Electrochem. Soc.*, **142**, 1859 (1995).
21. D. M. Pesko, K. Timachova, R. Bhattacharya, M. C. Smith, I. Villaluenga, J. Newman, and N. P. Balsara, "Negative transference numbers in poly(ethylene oxide)-based electrolytes." *J. Electrochem. Soc.*, **164**, E3569 (2017).
22. I. Villaluenga, D. M. Pesko, K. Timachova, Z. Feng, J. Newman, V. Srinivasan, and N. P. Balsara, "Negative stefan-maxwell diffusion coefficients and complete electrochemical transport characterization of homopolymer and block copolymer electrolytes." *J. Electrochem. Soc.*, **165**, A2766 (2018).
23. N. P. Balsara and J. Newman, "Relationship between steady-state current in symmetric cells and transference number of electrolytes comprising univalent and multivalent ions." *J. Electrochem. Soc.*, **162**, A2720 (2015).
24. A. Noda, K. Hayamizu, and M. Watanabe, "Pulsed-gradient Spin-Echo 1H and 19F NMR ionic diffusion coefficient, viscosity, and ionic conductivity of non-chloroaluminate room-temperature ionic liquids." *J. Phys. Chem. B*, **105**, 4603 (2001).
25. M. Gouverneur, F. Schmidt, and M. Schönhoff, "Negative effective li transference numbers in li salt/ionic liquid mixtures: does li drift in the 'wrong' direction?" *Phys. Chem. Chem. Phys.*, **20**, 7470 (2018).
26. K. Yoshida, M. Tsuchiya, N. Tachikawa, K. Dokko, and M. Watanabe, "Change from glyme solutions to quasi-ionic liquids for binary mixtures consisting of lithium bis(trifluoromethanesulfonyl)amide and glymes." *J. Phys. Chem. C*, **115**, 18384 (2011).
27. K. Ueno, K. Yoshida, M. Tsuchiya, N. Tachikawa, K. Dokko, and M. Watanabe, "Glyme-lithium salt equimolar molten mixtures: concentrated solutions or solvate ionic liquids?" *J. Phys. Chem. B*, **116**, 11323 (2012).
28. C. Zhang, K. Ueno, A. Yamazaki, K. Yoshida, H. Moon, T. Mandai, Y. Umebayashi, K. Dokko, and M. Watanabe, "Chelate effects in glyme/lithium bis(trifluoromethanesulfonyl)amide solvate ionic liquids. I. Stability of solvate cations and correlation with electrolyte properties." *J. Phys. Chem. B*, **118**, 5144 (2014).
29. F. Schmidt and M. Schönhoff, "Solvate cation migration and ion correlations in solvate ionic liquids." *J. Phys. Chem. B*, **124**, 1245 (2020).
30. L. M. Thieu, L. Zhu, A. G. Korovich, M. A. Hickner, and L. A. Madsen, "Multiscale tortuous diffusion in anion and cation exchange membranes." *Macromolecules*, **52**, 24 (2019).
31. B. E. Kidd, S. J. Forbey, F. W. Steuber, R. B. Moore, and L. A. Madsen, "Multiscale lithium and counterion transport in an electrospun polymer-gel electrolyte." *Macromolecules*, **48**, 4481 (2015).
32. C. D'Agostino, M. D. Mantle, C. L. Mullan, C. Hardacre, and L. F. Gladden, "Diffusion, ion pairing and aggregation in 1-Ethyl-3-methylimidazolium-based ionic liquids studied by 1H and 19F PFG NMR: effect of temperature, anion and glucose dissolution." *ChemPhysChem*, **19**, 1081 (2018).
33. M. C. Lonergan, D. F. Shriver, and M. A. Ratner, "Polymer electrolytes: the importance of ion-ion interactions in diffusion dominated behavior." *Electrochim. Acta*, **40**, 2041 (1995).
34. G. E. Murch, "The haven ratio in fast ionic conductors." *Solid State Ionics*, **7**, 177 (1982).
35. R. B. Bird, W. E. Stewart, and E. N. Lightfoot, *Transport Phenomena* (Wiley, New Jersey) (1960).
36. C. Schreiner, S. Zugmann, R. Hartl, and H. J. Gores, "Fractional walden rule for ionic liquids: examples from recent measurements and a critique of the so-called ideal KCl line for the walden plot." *J. Chem. Eng. Data*, **55**, 1784 (2010).
37. A. Pinkert, K. L. Ang, K. N. Marsh, and S. Pang, "Density, viscosity and electrical conductivity of protic alkanolammonium ionic liquids." *Phys. Chem. Chem. Phys.*, **13**, 5136 (2011).
38. M. Chintapalli, K. Timachova, K. R. Olson, S. J. Mecham, D. Devaux, J. M. DeSimone, and N. P. Balsara, "Relationship between conductivity, ion diffusion, and transference number in perfluoropolyether electrolytes." *Macromolecules*, **49**, 3508 (2016).
39. N. Boden, S. A. Leng, and I. M. Ward, "Ionic conductivity and diffusivity in polyethylene oxide/electrolyte solutions as models for polymer electrolytes." *Solid State Ionics*, **45**, 261 (1991).
40. K. Hayamizu, Y. Aihara, S. Arai, and W. S. Price, "Diffusion, conductivity and DSC studies of a polymer gel electrolyte composed of cross-linked PEO, gamma-butyrolactone and LiBF4." *Solid State Ionics*, **107**, 1 (1998).
41. V. Bocharova and A. P. Sokolov, "Perspectives for polymer electrolytes: a view from fundamentals of ionic conductivity." *Macromolecules*, **53**, 4141 (2020).
42. M. D. Galluzzo, J. A. Maslyn, D. B. Shah, and N. P. Balsara, "Ohm's law for ion conduction in lithium and beyond-lithium battery electrolytes." *J. Chem. Phys*, **151**, 020901 (2019).
43. B. L. Dewing, N. G. Bible, C. J. Ellison, and M. K. Mahanthappa, "Electrochemically stable, high transference number lithium bis(malonato)borate polymer solution electrolytes." *Chem. Mater.*, **32**, 3794 (2020).
44. K. M. Diederichsen, K. D. Fong, R. C. Terrell, K. A. Persson, and B. D. McCloskey, "Investigation of solvent type and salt addition in high transference number nonaqueous polyelectrolyte solutions for lithium ion batteries." *Macromolecules*, **51**, 8761 (2018).
45. Y. Lu, M. Tikekar, R. Mohanty, K. Hendrickson, L. Ma, and L. A. Archer, "Stable cycling of lithium metal batteries using high transference number electrolytes." *Adv. Energy Mater.*, **5**, 1402073 (2015).
46. P. Barai, K. Higa, and V. Srinivasan, "The electrochemical society impact of external pressure and electrolyte transport properties on lithium dendrite growth." *J. Electrochem. Soc.*, **165**, A2654 (2018).
47. J. Landesfeind and H. A. Gasteiger, "Temperature and concentration dependence of the ionic transport properties of lithium-ion battery electrolytes." *J. Electrochem. Soc.*, **166**, A3079 (2019).
48. J. T. Vardner, T. Ling, S. T. Russell, A. M. Perakis, Y. He, N. W. Brady, S. K. Kumar, and A. C. West, "Method of measuring salt transference numbers in ion-selective membranes." *J. Electrochem. Soc.*, **164**, A2940 (2017).
49. N. Craig, S. A. Mullin, R. Pratt, and G. B. Crane, "Determination of transference number and thermodynamic factor by use of anion-exchange concentration cells and concentration cells." *J. Electrochem. Soc.*, **166**, A2769 (2019).
50. J. Evans, C. Vincent, and P. Bruce, "Electrochemical measurement of transference numbers in polymer electrolytes." *Polymer*, **28**, 2324 (1987).
51. P. G. Bruce and C. A. Vincent, "Steady state current flow in solid binary electrolyte cells." *J. Electroanal. Chem.*, **225**, 1 (1987).
52. D. B. Shah, H. Q. Nguyen, L. S. Grundy, K. R. Olson, S. J. Mecham, J. M. DeSimone, and N. P. Balsara, "Difference between approximate and rigorously measured transference numbers in fluorinated electrolytes." *Phys. Chem. Chem. Phys.*, **21**, 7857 (2019).
53. D. W. Dees, V. S. Battaglia, L. Redey, G. L. Henriksen, R. Atanasoski, and A. Bélanger, "Toward standardizing the measurement of electrochemical properties of solid-state electrolytes in lithium batteries." *J. Power Sources*, **89**, 249 (2000).
54. K. R. Olson, D. H. C. Wong, M. Chintapalli, K. Timachova, R. Januszewicz, W. F. M. Daniel, S. Mecham, S. Sheiko, N. P. Balsara, and J. M. DeSimone, "Liquid perfluoropolyether electrolytes with enhanced ionic conductivity for lithium battery applications." *Polymer*, **100**, 126 (2016).
55. D. B. Shah, K. R. Olson, A. Karny, S. J. Mecham, J. M. DeSimone, and N. P. Balsara, "Effect of anion size on conductivity and transference number of perfluoroether electrolytes with lithium salts." *J. Electrochem. Soc.*, **164**, A3511 (2017).
56. D. H. C. Wong, J. L. Thelen, Y. Fu, D. Devaux, A. A. Pandya, V. S. Battaglia, N. P. Balsara, and J. M. DeSimone, "Nonflammable perfluoriether-based electrolytes for lithium batteries." *Proc. Natl. Acad. Sci. USA*, **111**, 3327 (2014).
57. E. O. Stejskal and J. E. Tanner, "Spin diffusion measurements: spin echoes in the presence of a time-dependent field gradient." *J. Chem. Phys.*, **42**, 288 (1965).
58. D. Sinnaeve, "The stejskal-tanner equation generalized for any gradient shape–an overview of most pulse sequences measuring free diffusion." *Concepts Magn. Reson., Part A*, **40**, 39 (2012).
59. A. Maitra and A. Heuer, "Cation transport in polymer electrolytes: a microscopic approach." *Phys. Rev. Lett.*, **98**, 227802 (2007).
60. M. Watanabe, S. Nagano, K. Sanui, and N. Ogata, "Estimation of Li + transport number in polymer electrolytes by the combination of complex impedance and potentiostatic polarization measurements." *Solid State Ionics*, **28–30**, 911 (1988).
61. V. K. Vanag and I. R. Epstein, "Cross-diffusion and pattern formation in reaction-diffusion systems." *Phys. Chem. Chem. Phys.*, **11**, 897 (2008).

62. J. C. Clunie, N. L. Burns, and J. K. Baird, "Nernst-hartley evaluation of the interdiffusion coefficient of aqueous nickel sulfamate using new measurements of the equivalent conductances of the ions." *J. Electroanal. Chem.*, **328**, 317 (1992).
63. A. Heintz, R. Ludwig, and E. Schmidt, "Limiting diffusion coefficients of ionic liquids in water and methanol: a combined experimental and molecular dynamics study." *Phys. Chem. Chem. Phys.*, **13**, 3268 (2011).
64. G. S. Hartley, *Philos. Mag.*, **12**, 473 (1931).
65. A. Einstein, "Investigations on the theory of brownian movement." *Leipzig, Ann. Phys.*, **17**, 549 (1905).
66. M. A. Vorotyntsev, V. A. Zinovyeva, and M. Picquet, "Diffusional transport in ionic liquids: stokes-einstein relation or 'sliding sphere' model ? Ferrocene (Fc) in imidazolium liquids." *Electrochim. Acta*, **55**, 5063 (2010).
67. J. F. Chambers, J. M. Stokes, and R. H. Stokes, "Conductances of concentrated aqueous sodium and potassium chloride solutions at 25C." *J. Phys. Chem.*, **60**, 985 (1956).